Non-photochemical laser-induced nucleation

Perspective: Non-photochemical laser-induced nucleation

Andrew J. Alexander[1, a)] and Philip J. Camp[1, 2, b)]
[1)] *School of Chemistry, David Brewster Road, Edinburgh EH9 3FJ, Scotland*
[2)] *Department of Theoretical and Mathematical Physics, Institute of Natural Sciences and Mathematics, Ural Federal University, 51 Lenin Avenue, Ekaterinburg 620000, Russia*

(Dated: 10 December 2018)

Non-photochemical laser-induced nucleation (NPLIN) is the formation of a new phase from a metastable phase by the action of light on matter. Using millijoule, nanosecond laser pulses at visible and near-infrared wavelengths, it is possible to form the new phase localized in the volume of the beam. In the case of nucleating molecular solids, the laser polarization may have an effect on the particular polymorph that is formed. Despite the huge potential for applications of NPLIN, there is uncertainty regarding the molecular-scale mechanism, and various possible scenarios may well be relevant to nucleation in general, and not just NPLIN. In this Perspective, the discovery and phenomenology of NPLIN are described, putative mechanisms are outlined, and some observations on the broader class of nucleation phenomena are given.

I. INTRODUCTION

Nucleation is the starting point in the formation of a new phase of a substance from another, e.g., the formation of solid ice from liquid water. It occurs throughout nature, such as in the formation of clouds in the atmosphere, and biomineralization of bones and shells of animals. Nucleation also has tremendous economic significance in manufacturing and processing high-value materials such as pharmaceuticals, pigments, and ingredients for food. Much has yet to be unraveled about the molecular-scale mechanisms and underlying dynamics of nucleation. Through studying the chemical physics of nucleation we strive to build a richer appreciation, and achieve deeper control, of this essential process.

Primary nucleation occurs spontaneously in the absence of any of the new phase, while *secondary nucleation* is induced by an amount of preexisting material.[1] Heterogeneous primary nucleation occurs at an inert surface, while homogeneous primary nucleation occurs in the bulk. This Perspective is focused mainly on the primary nucleation of solids from solution, and so the terminology used will be appropriate to that case. The thermodynamic driving force for nucleation is the chemical potential μ of solute molecules. When the chemical potential in a solid (μ_1) is lower than that in the solution (μ_0) the system is said to be supersaturated. At saturation, $\mu_1 = \mu_0$, and the concentration of the solute is equal to the solubility c_s. The degree of supersaturation is measured by parameter $S = c/c_\mathrm{s}$. A supersaturated solution ($S > 1$, $\mu_1 < \mu_0$) may exist in a metastable state, kinetically stabilized by a free-energy barrier arising from the (positive) interfacial free energy between the solid phase and the surrounding solution.

Two very general models are currently used to describe nucleation. The longest standing approach is *classical nucleation theory* (CNT), based on the work of Gibbs, Becker and Döring, and many others.[2] A full discussion of CNT lies outside the scope of this perspective, but in terms of mechanism, it describes the fate of a solid cluster formed randomly in solution by the aggregation of molecules. The number of such clusters is dictated by the free energy change of formation from solution, and this is expressed in terms of interfacial and bulk contributions. The total free-energy change of formation of a solid particle is written

$$\Delta G = s\gamma + v\rho\Delta\mu \tag{1}$$

where s is the surface area of the particle, γ is the interfacial tension between particle and solution, v is the volume of the particle, ρ is the number of molecules per unit volume in the solid phase, and $\Delta\mu = \mu_1 - \mu_0$. The number of molecules in the cluster is $n = \rho v$. For small clusters, the positive interfacial free energy outweighs the negative bulk free energy, while the opposite is true for large clusters, and so a free-energy maximum occurs at some critical cluster size. A plot of $\Delta G(r)$ for spherical particles of radius r is shown in Fig. 1. The rate of nucleation is dictated by the height of the free-energy barrier, and the rate of accretion of molecules onto particles near the top of the barrier. Small clusters on one side of the barrier are likely to redissolve, while large clusters on the other side of the barrier are likely to grow. The central assumption of CNT is that nucleation and growth are described in terms of a single 'reaction coordinate' or order parameter, this being the number of molecules in the cluster. Commonly, the solid clusters are considered to be spherical (to minimize the surface area-to-volume ratio) and bulk values of γ, ρ, and μ are assumed. An example is detailed in Section III B.

A more elaborate description of crystallization is given by the *two-step nucleation* (TSN) model.[3] The key difference from CNT is that there are two (perhaps more) barriers in the free-energy profile. The first barrier separates two states, one being the solute in solution, and the other being the solute in the form of non-crystalline clusters; these lack long-range structural order, perhaps contain solvent, and are sometimes referred to as being in a liquid-like or dense-liquid amorphous phase. The second barrier separates amorphous clusters from crystalline clusters. Hence, the free-energy surface is described in

[a)] Electronic mail: andrew.alexander@ed.ac.uk
[b)] Electronic mail: philip.camp@ed.ac.uk

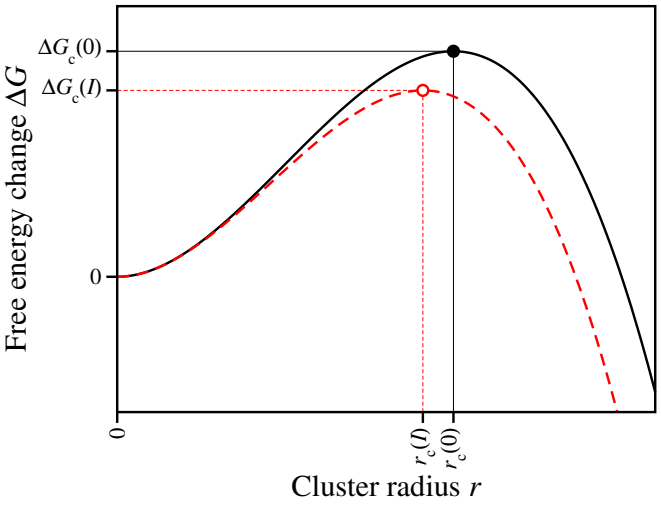

FIG. 1. Free energy of forming a spherical solid cluster of radius r from solution without (black solid line) and with (red dashed line) irradiation with laser light of intensity I, according to CNT and the dielectric polarization model (described in Section III B). The critical radius and barrier height (r_c, ΔG_c) in both cases are indicated by the points. The reductions in r_c and ΔG_c are not shown to scale.

terms of two order parameters, the cluster size and the degree of crystallinity. The early stage of the process is mainly one of growth of the amorphous cluster, and the late stage is mainly the development of crystalline order. Much of the strongest evidence for dense-liquid clusters has come from studies of protein nucleation: evidence in the case of ionic or small-molecule systems is sparse,[4] perhaps with the exception of $CaCO_3$.[5]

The concepts outlined above can be applied to other kinds of nucleation. For example, the crystallization of a solid from its melt can be described in terms of the degree of supercooling below the freezing temperature, and the vaporization of a liquid can be expressed in terms of the degree of superheating above the boiling temperature.

The greatest challenge for studying primary nucleation is its stochastic nature. Even if the right thermodynamic conditions are provided, e.g., by supercooling a liquid below its freezing temperature, there is no guarantee nucleation will take place. In general, it is not possible to control the time, location, or morphology of the new phase that is nucleated. Any technique for inducing nucleation that can offer some degree of control would be very useful. Several methods have been developed that make use of external perturbations such as mechanical shock,[6] electric fields or discharges,[7,8] high-power ultrasound,[9] and more recently, laser light.[10–12]

Non-photochemical laser-induced nucleation (NPLIN) involves using short (usually nanosecond) laser pulses to trigger crystallization. A typical NPLIN experiment is illustrated in Fig. 2 (Multimedia view), and a movie is available online. Figure 2 shows the effect of a single 5-ns laser pulse incident on a supersaturated aqueous solution of ammonium chloride. The path of the laser beam can be seen clearly by the crystals that are nucleated, which begin to grow and sediment.

As will be discussed in this Perspective, NPLIN offers

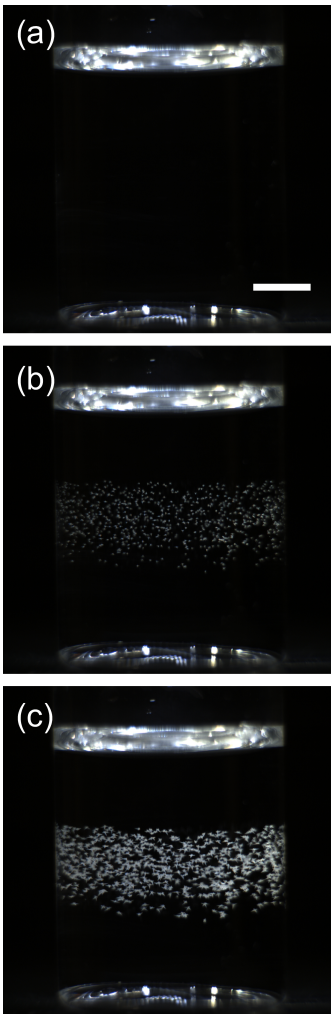

FIG. 2. (Multimedia view) Images of NPLIN obtained with a single laser pulse (5 ns, 532 nm) incident on a glass vial of supersaturated ammonium chloride in water ($S = 1.25$ at 19.5 °C). Sequence shown at times (a) 0 s, (b) 1 s, and (c) 2 s after the laser pulse. The width of the laser beam was approximately 0.7 cm and the pulse energy was 100 mJ. The scale bar in (a) represents 0.5 cm. A movie of this example is available online.

several advantages over other nucleation methods: (i) it offers temporal control of nucleation through the time and duration of the laser pulse; (ii) it offers spatial control of nucleation through the shape, size, and pathway of the laser beam; (iii) the wavelength and intensity of the laser pulse are chosen so that there is no photochemical damage to the system; and (iv) the perturbation can be applied to closed systems at a distance. Nonetheless, the application of NPLIN is subject to some caveats: (i) the components must have low optical absorbances, so as to avoid heating or photochemical damage; (ii) there are practical limits to the volume of the system that can be exposed to the laser light; and (iii) some systems just do not undergo NPLIN.

By offering unprecedented spatial and temporal control, NPLIN can be used to investigate nucleation mechanisms. Because NPLIN in closed systems can be triggered remotely, it is possible to probe regions of the phase

diagram that may not be accessible by other means. For example, it may be possible to access new polymorphs, solvates, and co-crystals at extreme pressures and temperatures, or in unusual confined matrices. This would have clear benefits in applications where the phase of a material is important, for example, in active pharmaceutical ingredients.

This Perspective is arranged as follows. Section II is a brief introduction to the phenomenology of NPLIN with an historical perspective. On the whole, this will focus on the use of pulsed lasers for NPLIN, as developed by Garetz and co-workers.[10] For discussion of crystal nucleation due to trapping with focused continuous-wave (CW) laser light, the reader is directed elsewhere.[12,13] Questions arising from the experimental observations, and the mechanisms proposed subsequently, are discussed in Section III. The connections between NPLIN and other physical methods of inducing nucleation are discussed in Section IV. Section V offers some possible directions for future research.

II. NON-PHOTOCHEMICAL LASER-INDUCED NUCLEATION

A. Phenomenology

NPLIN was discovered by chance in the mid-1990s, while Garetz *et al.* were attempting to study second-harmonic generation in aqueous supersaturated solutions of urea $(NH_2)_2CO$.[10,14] On exposing solutions to nanosecond pulses of near-infrared (1064 nm) laser light, they found that needle-shaped crystals of urea were formed. The duration of each pulse was short (20 ns) and the rate of pulses was low (10 s^{-1}). Heating due to the laser light was ruled out as the cause, because the absorption of water is small (0.14 cm^{-1}) at this wavelength.[15] There are no electronic absorption bands of urea accessible in the near-infrared region. Multiphoton absorption was considered to be unlikely because unfocused pulses were used (100 mJ $pulse^{-1}$, 0.02 cm^2) so that the resulting peak power density was low (250 MW cm^{-2}). The term *non-photochemical* was applied to distinguish the effect from previous studies where light, typically in the ultraviolet region of the spectrum, causes precipitation of droplets or particles.[16,17] It is fair to say that the mechanisms of both photochemical and non-photochemical nucleation are not well understood at present, and some putative NPLIN mechanisms will be described in Sections III and IV.

In experiments on urea solutions, Matic *et al.* observed that there was a threshold laser power to NPLIN, and that the fraction of samples nucleated increased with peak laser power above that threshold.[18] Linearly polarized (LP) light was more effective than circularly polarized (CP) light, but there was no clear dependence on wavelength (532 versus 1064 nm).[19] The most significant initial observation concerning NPLIN was that the needles of urea were aligned with the direction (horizontal or vertical) of the electric field of LP light. The CO bond direction is the most polarizable axis of the molecule, which in the crystal lies parallel to the long axis of the needle. This prompted the idea that the molecules were being aligned along the direction of the electric field of the light, similar to the optical Kerr effect (OKE) in liquids.[20–24] The period of the electric field of the light ($\sim 10^{-14}$ s) is much shorter than the molecular rotation time in solution, and so it cannot align the permanent dipole moment of urea. Alignment might take place through interaction with the anisotropic electronic polarizability of the molecule, which is discussed in Section III A. Note, though, that recent experiments show no evidence for alignment of needle-shaped crystals of urea with respect to the direction of the electric field of LP light.[25]

In these early studies, it was suggested that for NPLIN to work, the solutions needed to be aged (approximately 4 to 8 days) before exposure to the laser light. This observation was explained as the requirement for time to grow a population of large, sub-critical clusters.[26] Later studies have shown that aging is not a *requirement* for NPLIN, although it can influence the nucleation probability.[25,27–29]

B. Polarization switching

Following on from the first work on urea, experiments on aqueous glycine showed that NPLIN favored nucleation of the γ polymorph, whereas spontaneous nucleation under similar conditions always produced the α polymorph.[26] Further study showed that LP light produced γ-glycine and CP light produced α-glycine.[30] The effect was termed *polarization switching*. This remarkable result suggested that polymorphism could be controlled simply by changing the polarization of the light, without having to use crystal seeds.[31] The polarization-switching effect was explained in terms of the shape of the polarizability anisotropy of the molecular units that make up the crystal. Looking at the crystal structure of γ-glycine, the main structural motif consists of helical chains of glycine molecules having an overall rod-shaped polarizability.[30] Garetz *et al.* noticed that chains of molecules with this structure might be obvious precursors for γ-glycine in solution, and such chains would be aligned to a greater degree by LP light than by CP light. In contrast, the crystal structure of α-glycine consists of planes of dimers, and it was supposed that this planar arrangement would interact preferentially with CP light. The idea is illustrated in Fig. 3, which shows complete formula units in supercells of the two polymorphs of glycine. α-glycine[32] has no rod-like structural motifs, whereas γ-glycine[33] contains a motif consisting of three staggered chains of molecules.

The early experimental indications of the requirement for aging, the alignment of urea needles, and polarization switching of glycine appeared to fit in well with both the TSN model and the OKE mechanism proposed for NPLIN. The idea was that the non-crystalline clusters in the TSN model were susceptible to interaction with the peak electric field of the pulsed laser light such that they would rearrange and become viable crystal nuclei. So far, so good with explaining NPLIN.

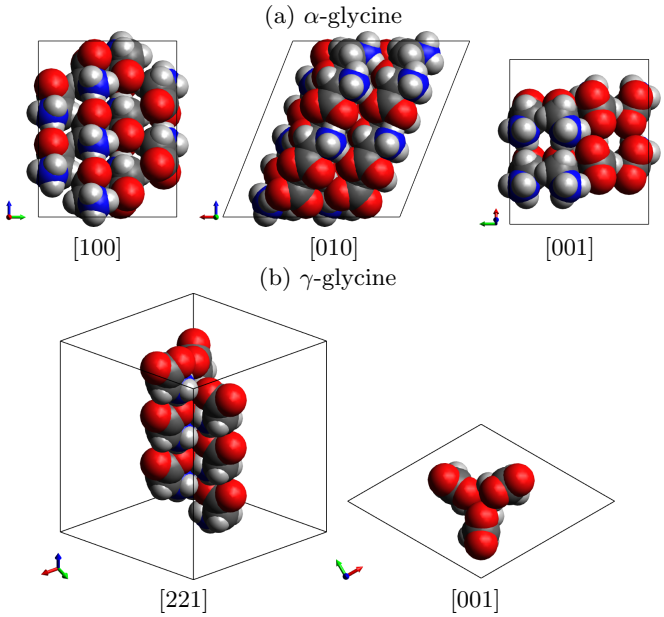

FIG. 3. Structural motifs in crystals of glycine. (a) A $3\times1\times3$ supercell of α-glycine[32] viewed along the [100], [010], and [001] directions. (b) A $2\times2\times4$ supercell of γ-glycine[33] viewed along the [221] and [001] directions. The coloring scheme is H (white), C (gray), N (blue), and O (red). In all cases, only the complete formula units within the supercell are shown. The red, green, and blue axes are the Cartesian x, y, and z axes, respectively. (Figure prepared using *Avogadro*.[34,35])

C. NPLIN of halide salts

The work of Garetz *et al.* was brought to the attention of one of us (AJA) in 2000, when Brian Bean, a graduate student in Dick Zare's group at Stanford University, was investigating crystallization of amino acids using circularly polarized light. It was difficult to obtain control of the solution conditions, and so the experiments were not continued.[36] Fast-forward to 2006, and the first system studied in detail in Edinburgh was aqueous potassium chloride (KCl). Supersaturated solutions (S = 1.05–1.10) exposed to laser pulses yielded visible crystals within a few minutes. At the lowest laser powers (above a threshold) it was observed that a single crystal could be produced with a single laser pulse. Therefore, whatever the mechanism, nucleation was determined within the duration of the laser pulse (7 ns). A mean threshold laser power of 6.4 MW cm^{-2} (0.26 cm^2 beam) was observed. One of the possible explanations for the threshold might have been the effect of the sample container. However, no difference in threshold was seen for polymethylpentene (PMP) vessels as compared to borosilicate glass. A threshold power was later observed by Fang *et al.* in levitated droplets of aqueous KCl, i.e., with *no* container![37]

As expected, solutions with higher supersaturations were more susceptible to nucleation, or more 'labile' for short.[28] Solutions of KCl at fixed supersaturation (S = 1.06) were found to be more labile at 33 °C than at 23 °C. This was attributed to the higher absolute concentration of solute at the higher temperature.[38] At low laser powers, for both aqueous KCl and KBr, the probability of nucleation increased linearly with respect to the peak laser power, which scales as the square of the electric field strength. The probability of nucleation tended towards unity at high laser powers. KBr was found to be a factor of two more labile than KCl, but the effects of wavelength were mixed.[38] A comparison of short (6 ns) versus long (200 ns) nanosecond pulses suggested that the nucleation probability was proportional to the peak laser power rather than the total pulse energy.[39]

In order to investigate spatial localization of crystal growth, Duffus *et al.* nucleated KCl crystals in an agarose gel by raster scanning the system with single laser pulses.[40] Because of the reduced solute diffusion in the gel, nucleated crystals did not continue growing beyond a millimetre or so, and therefore a controlled spatial distribution of microcrystals could be produced in the gel matrix. Even greater control over nucleation was demonstrated by using an evanescent (non-propagating) wave to produce KCl crystals within 100 nm of a glass-solution interface.[41]

One of the early questions to be addressed was whether impurities or dust affected NPLIN. Solutions were prepared with 0.2 μm-pore filters, high-purity KCl and water, careful cleaning, and even preparation in an enclosed glove box with filtered nitrogen atmosphere. It was concluded that solid impurities (larger than 200 nm) were not needed for NPLIN in this system, but that unfiltered samples were clearly more labile to nucleation.[28] Later experiments showed that purposely doping aqueous ammomium chloride solutions with iron-oxide nanoparticles led to an increase in NPLIN lability.[42] This will be discussed further in Section III C.

Since the crystal structure of KCl is cubic, there is no preferred axis for alignment, which rules out the OKE mechanism. Moreover, no dependence on laser polarization was observed.[28] For these reasons, an alternative mechanism based on dielectric polarization (DP) of solute clusters was developed, which shall be discussed in more detail in Section III B.

D. NPLIN of other systems

The early work on urea, glycine, and halide salts, led to the application of NPLIN to many other systems. A good summary of the work up to 2014 has been given by Clair *et al.*,[43,44] but some of the important findings are outlined here.

Moving beyond aqueous solutions, a phase change from isotropic to nematic in a supercooled liquid crystal was demonstrated using picosecond (45 ps) laser pulses.[45] Nucleation of gas bubbles in supersaturated aqueous solutions of carbon dioxide (CO_2) has been studied.[41,46] NPLIN in single-component systems has also been demonstrated, in glacial acetic acid[47] and in molten sodium chlorate.[48]

Looking to develop NPLIN to more-complex systems, Garetz *et al.* demonstrated NPLIN of hen egg-white lysozyme protein, noting that picosecond laser pulses (100 ps) were more effective than nanosecond pulses

(5 ns).[49] It was believed that the picosecond pulses offered higher peak powers at lower pulse energies, and therefore less heating of the solution droplets. Yennawar *et al.* used a screening method in conjunction with NPLIN to investigate protein nucleation. For most proteins they found that NPLIN produced significant improvements in crystal quality, size, growth time, and diffraction resolution. They also nucleated some proteins under screening conditions where the control did not crystallize.[50]

Arciniegas *et al.* have used NPLIN to produce methylammonium lead halide ($CH_3NH_3PbX_3$, X = Cl, Br, or I) perovskite crystals from simple precursors on a Si substrate.[51] This is significant not only because of the complexity of the crystalline product, but also because the laser parameters, such as intensity and duration, control the sizes of the crystalline particles, ranging from 0.5–50 μm.

Liu and Liu have examined the nucleation of hematite (α-Fe_2O_3) crystals using nanosecond laser pulses.[52] Depending on the pulse energy, amorphous, crystalline, or both types of particles could be formed. This was interpreted in terms of the TSN model. With low pulse energies, the first barrier separating solution and amorphous states was overcome, leading to the formation of an amorphous particle, which later converts in to a crystalline particle. With high pulse energies, both barriers separating solution and crystalline states are overcome simultaneously, leading to the direct formation of crystalline particles.

Some studies have employed high-power conditions, where the pulsed light induces nucleation by a photochemical or laser-induced cavitation mechanism. These conditions can be achieved by focusing a pulsed laser, typically through a microscope objective, or through use of femtosecond laser pulses.[11,53,54]

Of particular interest are studies aimed at clarifying the extent of polarization switching.[45] Experiments on aqueous L-histidine showed that the A polymorph was favored by CP light, whereas LP light produced a mixture of A and B polymorphs.[55] The results were rationalized in terms of the OKE mechanism, noting that the structural motifs of the crystal polymorphs possess rod-shaped and disk-shaped polarizabilities. Ikni *et al.* found that for carbamazepine dissolved in acetonitrile, form I was nucleated when using LP but not CP light, and that the effect disappeared with methanol as the solvent.[44] NPLIN of sulfathiazole in water-ethanol mixtures showed a preference for form IV with LP light, and form III with CP light.[56]

For glycine, the polarization switching has become less certain. Sun *et al.* found that the effect was limited to narrow windows of supersaturation and temperature.[19] A number of other attempts to reproduce the polarization switching effect have met with limited success, to the point that it is not clear if the effect occurs at all.[29,43,57]

In their work on glycine, Clair *et al.* passed the laser beam vertically downwards through the meniscus,[43] in contrast to previous NPLIN experiments where solutions were irradiated through the side of a vessel, i.e., the glass–solution interface.[19] They observed that some crystals nucleated at or near the air–solution interface, with morphologies of α-glycine distinct from the typical rod-shaped crystals obtained by spontaneous nucleation. It remains unknown whether the crystal morphology is due to the effects of the interface on the nucleation mechanism, the early-stage growth process, or both.

A complementary strand of research into laser-induced nucleation, pioneered by Masuhara, Sugiyama and coworkers, involves focusing a CW laser at the liquid–vapor interface of a thin film of solution.[53] The results have been explained in terms of optical trapping of the solute molecules, and appears to be preceded by formation of a dense-liquid phase prior to nucleation.[12,58] In these experiments even *undersaturated* solutions can be induced to nucleate solid while the optical field is present. With glycine solutions, an effect similar to polarization switching was observed, but with CP light favoring γ-glycine, opposite to NPLIN experiments. This was interpreted in terms of more-efficient trapping of clusters with disk-shaped polarizability by CP light. Disk-shaped clusters would normally be expected to favor α-glycine, but the trapping is believed to cause a significant local increase in S that leads to the γ polymorph.[59]

E. Summary

The discovery of NPLIN, and some of the subsequent experimental work, has been outlined in the preceding Sections. The effect can be summarized with the following key observations: (i) a minimum, threshold laser power is required for nucleation; (ii) the probability of nucleation increases with supersaturation, and scales linearly with low peak laser powers; (iii) the effect is not strongly wavelength dependent; (iv) a single, nanosecond laser pulse can induce nucleation; (v) the polarization of light affects the crystal product; (vi) aging of solutions appears to make NPLIN more effective, at least for some systems; and (vii) nanoparticle impurities increase the probability of NPLIN. These observations place a lot of demands on a complete theory of NPLIN, and it is likely that no single model can describe all of the phenomena. Nonetheless, some of the likely ingredients have been identified since the NPLIN phenomenon was discovered, and these are outlined in Section III.

III. MECHANISM

A. Optical Kerr effect

The OKE mechanism is considered here in more detail. Sun *et al.* described the alignment along laboratory-fixed coordinates ($i = x, y, z$) using three order parameters $K_i = \langle \cos^2 \theta_i \rangle$, where θ_i is the angle between a molecular axis and a laboratory axis.[60] They assumed a molecule with a uniaxial, ellipsoidal polarizability tensor, with diagonal elements α_a and $\alpha_b = \alpha_c$. When $\Delta\alpha = \alpha_a - \alpha_b > 0$ the polarizability ellipsoid is prolate ('rod-like'). When $\Delta\alpha < 0$ the polarizability ellipsoid is oblate ('disk-like'). For light linearly polarized (LP) along the x direction and traveling in the z direction, the

order parameters can be written approximately as[27,60]

$$K_i^{\mathrm{LP}} = \frac{1}{3} + \frac{s_i E^2 \Delta\alpha}{90 k_{\mathrm{B}} T} \tag{2}$$

where $s_x = 2$, $s_y = s_z = -1$, E is the electric field strength, k_{B} is Boltzmann's constant, and T is the temperature. The values of K_i range from 0 to 1, with 1 indicating maximal alignment along a particular direction. The parameters are mutually dependent due to the constraint that $K_x + K_y + K_z = 1$. For an isotropic distribution of molecules $K_i = \frac{1}{3}$, while the ground-state alignments in the rod-like and disk-like cases give $(K_x = 1, K_y = K_z = 0)$ and $(K_x = 0, K_y = K_z = \frac{1}{2})$, respectively. Similar equations apply for the case of circularly polarized (CP) light in the xy plane, where in particular, $s_x = s_y = 1/2$, and $s_z = -1$.[60] The key point is that LP light aligns rods better than disks, and CP light aligns disks better than rods.

The glaring problem with Eq. (2) is that significant alignment of the molecules is barely achievable with realistic electric fields. For glycine, $\Delta\alpha = 1.8 \times 10^{-40}$ C m^2 V^{-1}. With a typical laser intensity, the electric field is $E = 3 \times 10^7$ V m^{-1}, and the ratio of the interaction energy $\frac{1}{2}E^2\Delta\alpha$ to the thermal energy $k_{\mathrm{B}}T$ at 298 K is 2×10^{-5}.[60] To counter this, it was argued that molecules could act co-operatively within clusters to give an effectively higher interaction energy.[31] To investigate this possibility, Knott *et al.* used Monte Carlo simulations of a Potts model accommodating CNT and TSN scenarios.[61] In this model, each lattice site contained an occupancy variable (solute or solvent) and a 6-state orientation variable. It was found that an applied field reduced the free-energy barrier to nucleation through an orientational bias, and hence facilitated nucleation as in the CNT scenario. In addition, the field encouraged the crystallization of amorphous precritical clusters, as in the TSN mechanism. Unfortunately, the magnitudes of the field required (characterized by the site-field interaction parameter) were significantly higher than those used in experiments.

B. Dielectric polarization

As noted in Section II C, the crystal symmetry of simple halide salts such as KCl requires a different mechanism than the OKE for the interaction between the laser pulse and the solution. One such mechanism involves the dielectric response of the solution. Since the wavelengths of the laser light used in NPLIN are far from any absorption bands for the solute and solvent, the action of the electric field E of the laser is to polarize the electrons in the constituent atoms. A result from classical electromagnetism is that, for a homogeneous dielectric body with relative permittivity ϵ_{p} immersed in a homogeneous dielectric continuum with relative permittivity ϵ_{s}, the free energy is changed in the presence of the field by an amount proportional to $v(\epsilon_{\mathrm{p}} - \epsilon_{\mathrm{s}})E^2$, where v is the volume of the region.[62,63] Within the framework of CNT, the dielectric body is a precritical solid cluster, the dielectric continuum is the surrounding solution, and the relative permittivities $\epsilon = \epsilon(\omega)$ are those at the frequency of the laser radiation. Commonly, $\epsilon_{\mathrm{p}} > \epsilon_{\mathrm{s}}$ and so the effect of the field is to stabilize the body with respect to the solution. This is referred to as the dielectric polarization (DP) model.

Now the details of Eq. (1) can be fleshed out. For explicit calculations, it is necessary to assume a shape for the precritical cluster, which shall be taken as a sphere with radius r. At the saturation concentration, $\mu_1 = \mu_0 \simeq \mu_0^{\ominus} + k_{\mathrm{B}}T \ln(c_{\mathrm{s}}/c^{\ominus})$, and hence at other concentrations $\mu_1 - \mu_0 \simeq -k_{\mathrm{B}}T \ln S$. Rather than representing the laser radiation by its field E, it is more convenient to use the intensity $I = \frac{1}{2}\epsilon_0 c E^2$, where ϵ_0 is the vacuum permittivity, and c is the speed of light. Including the dielectric polarization term, the free energy change of cluster formation becomes

$$\Delta G(r, I) = 4\pi r^2 \gamma - \frac{4}{3}\pi r^3 \left(\rho k_{\mathrm{B}} T \ln S + aI\right) \tag{3}$$

where the coefficient a contains the dielectric contrast between the precritical cluster and the solution:

$$a = \frac{3\epsilon_{\mathrm{s}}(\epsilon_{\mathrm{p}} - \epsilon_{\mathrm{s}})}{c(\epsilon_{\mathrm{p}} + 2\epsilon_{\mathrm{s}})}. \tag{4}$$

The free-energy profile contains a maximum at

$$r_{\mathrm{c}}(I) = \frac{2\gamma}{\rho k_{\mathrm{B}} T \ln S + aI} \tag{5}$$

$$\Delta G_{\mathrm{c}}(I) = \frac{16\pi\gamma^3}{3(\rho k_{\mathrm{B}} T \ln S + aI)^2} \tag{6}$$

and hence the laser light leads to a reduction in both the critical radius r_{c} and the barrier height ΔG_{c}. This is sketched in Fig. 1, but not to scale; see below for the precise enumeration. Prior to the laser pulse, it may be assumed that all of the solid particles in the metastable solution (with $S > 1$) are smaller than the critical radius $r_{\mathrm{c}}(0)$, otherwise nucleation would already have been observed. In the presence of the laser pulse, $I > 0$, and those clusters in the range $r_{\mathrm{c}}(I) < r < r_{\mathrm{c}}(0)$, which were previously precritical, are supercritical; see Fig. 1. Therefore, if it is assumed that this subset of preexisting, precritical clusters will go on to form viable crystals, then the probability of nucleation (as defined in terms of numbers of visible crystals) can be computed. To see this, the average number of precritical clusters in the metastable solution is given by

$$N_{\mathrm{cluster}} = \frac{N_{\mathrm{molecule}}}{\langle n \rangle} \tag{7}$$

where N_{molecule} is the total number of solute molecules (or formula units in the case of a salt) in the volume of the laser beam, and

$$\langle n \rangle = \frac{4\pi\rho\langle r^3 \rangle}{3} = \frac{4\pi\rho}{3} \times \frac{\int_0^{r_{\mathrm{c}}(0)} r^3 e^{-\Delta G(r,0)/k_{\mathrm{B}}T} \mathrm{d}r}{\int_0^{r_{\mathrm{c}}(0)} e^{-\Delta G(r,0)/k_{\mathrm{B}}T} \mathrm{d}r} \tag{8}$$

is the average number of molecules in a cluster. The number of clusters that go on to form viable crystals is

$$N_{\mathrm{crystal}} = N_{\mathrm{cluster}} \times \frac{\int_{r_{\mathrm{c}}(I)}^{r_{\mathrm{c}}(0)} e^{-\Delta G(r,0)/k_{\mathrm{B}}T} \mathrm{d}r}{\int_0^{r_{\mathrm{c}}(0)} e^{-\Delta G(r,0)/k_{\mathrm{B}}T} \mathrm{d}r}. \tag{9}$$

Putting these equations together yields the following prediction for the average number of viable crystals.

$$N_{\text{crystal}} = \frac{3N_{\text{molecule}}}{4\pi\rho} \times \frac{\int_{r_c(I)}^{r_c(0)} e^{-\Delta G(r,0)/k_B T} \mathrm{d}r}{\int_0^{r_c(0)} r^3 e^{-\Delta G(r,0)/k_B T} \mathrm{d}r}. \quad (10)$$

In the experiments, the probability of nucleation $p_{\text{nucleation}} = 1 - p_0$, where p_0 is the probability that no viable crystals are observed in any of the (very many) repeat experiments carried out with separate vials of solution. From the Poisson distribution, $p_0 = \exp(-N_{\text{crystal}})$, where N_{crystal} is emphasized as the *average* number of viable crystals.

The stabilizing effect of the laser field is very small, but it has a substantial effect on the probability of observing viable crystals, as will now be demonstrated. As a concrete example, consider the parameters given in Table I for KCl(aq) with $S = 1.060$ at $T = 296.15$ K, shot with a 1064 nm laser pulse with a typical intensity $I = 15$ MW cm^{-2}.[38] The ratio $aI/\rho k_B T \ln S \sim 10^{-5}$, and the reductions in the critical radius and barrier height are only 0.005% and 0.01%, respectively. With these observations, it is easy to explain the dependence of $p_{\text{nucleation}}$ on I. Firstly, since $r_c(0) - r_c(I) \ll r_c(0)$, the integral in the numerator of Eq. (10) can be approximated by

$$\int_{r_c(I)}^{r_c(0)} e^{-\Delta G(r,0)/k_B T} \mathrm{d}r \approx e^{-\Delta G_c(0)/k_B T} \left[r_c(0) - r_c(I)\right]. \quad (11)$$

Secondly, since $aI \ll \rho k_B T \ln S$,

$$r_c(0) - r_c(I) \approx \frac{2\gamma a I}{(\rho k_B T \ln S)^2}. \quad (12)$$

Hence, $N_{\text{crystal}} = mI$ and $p_{\text{nucleation}} = 1 - \exp(-mI)$, where m is a 'lability' constant independent of the laser intensity.

$$m = \frac{3N_{\text{molecule}}\gamma a}{2\pi\rho^3 (k_B T \ln S)^2} \times \frac{e^{-\Delta G_c(0)/k_B T}}{\int_0^{r_c(0)} r^3 e^{-\Delta G(r,0)/k_B T} \mathrm{d}r} \quad (13)$$

As explained in Section II, NPLIN experiments show that there is a threshold laser intensity, $I_{\text{threshold}}$, of as-yet-unknown origin. It turns out that simply shifting the CNT prediction yields excellent agreement with experimental results. Figure 4 shows the function $p_{\text{nucleation}} = 1 - \exp[-m(I - I_{\text{threshold}})]$ along with experimental data for aqueous potassium-halide solutions with $S = 1.060$, nucleated at different temperatures and with different laser wavelengths.[38] For the specific case given in Table I, the experimentally measured lability is $m = 0.055 \pm 0.003$ MW^{-1} cm^2. The only fitted parameter in Eq. (13) is the interfacial tension γ, and independent measurements of this quantity vary wildly (0.98–169 mJ m^{-3}).[64] In the vicinity of the threshold laser intensity, the DP model predicts correctly that $p_{\text{nucleation}} \approx m(I - I_{\text{threshold}})$.[28] The agreement between the shifted theory and experiment is good, but it must be emphasized that the theory does not offer an explanation for this threshold.

The DP model has been tested thoroughly,[28,38,40] and it can be used to rationalize all of the main variations of $p_{\text{nucleation}}$ with temperature, supersaturation, and solute and wavelength (through the dielectric-contrast parameter a). The origin of the threshold intensity is still unknown, although it has nothing to do with the solution container, because levitated droplets of supersaturated solution show the same effect.[37]

One aspect of NPLIN that has not been addressed yet is the laser pulse duration. Knott *et al.* predicted theoretically that 10-ns laser pulses are too short for clusters to assemble purely from monomers.[65] In experiments on aqueous potassium chloride solutions, the probability of nucleation was seen to depend only on the peak intensity, and not the total duration and hence the total energy.[39] In unpublished work on the same system, 5 ps pulses did not cause NPLIN, while 100 ps and longer pulses

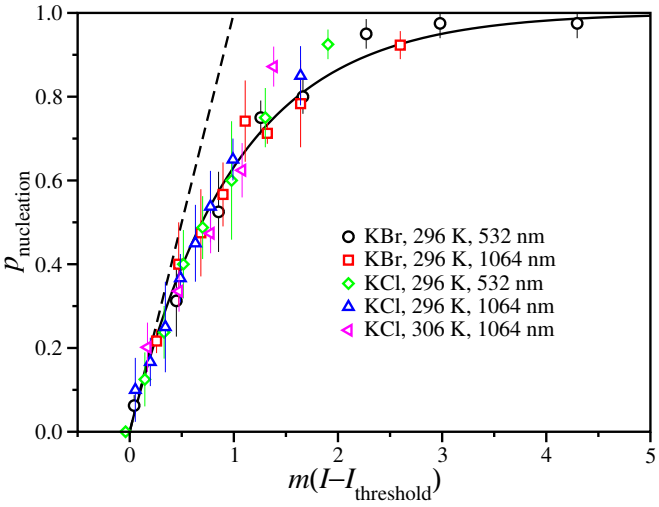

FIG. 4. Probability of nucleation $p_{\text{nucleation}}$ as a function of laser intensity expressed in the form $m(I - I_{\text{threshold}})$. The solid line is the prediction of the DP model, and the dashed line shows the initial linear dependence. The points are experimental data for aqueous potassium-halide solutions with $S = 1.060$.[38]

TABLE I. Physical and derived parameters for aqueous potassium-chloride solutions with $S = 1.060$ at $T = 23$ °C, nucleated using 1064 nm laser light with $I = 15$ MW cm^{-2}.[38] The symbols are defined in the text.

γ	5.283×10^{-3} J m^{-3}
ρ	1.603×10^{28} m^{-3}
ϵ_p(1064 nm)	2.189
ϵ_s(1064 nm)	1.754
$\rho k_B T \ln S$	3.8×10^6 J m^{-3}
$r_c(0)$	2.8 nm
$\Delta G_c(0)/k_B T$	41
I	15×10^{10} W m^{-2}
aI	200 J m^{-3}
$r_c(0) - r_c(I)$	1.5×10^{-4} nm
$[\Delta G_c(0) - \Delta G_c(I)]/k_B T$	4.4×10^{-3}
$\int_0^{r_c(0)} r^3 e^{-\Delta G(r,0)/k_B T} \mathrm{d}r$	2.4×10^{-39} m^4
N_{molecule}	8.9×10^{20}
m	5.5×10^{-12} W^{-1} m^2

did. Atomistic molecular-dynamics (MD) simulations of amorphous clusters in metastable, supersaturated aqueous potassium chloride solutions show that the *average* size is at least 10 ions at saturation, and that the reorganization time (measured by the lifetimes of ions within clusters) was in the region of 40–100 ps, depending on concentration.[66] Moreover, the nature of the single-ion dynamics in highly clustered solutions is 'glassy', with strong signatures of the cooperative motion evident in the self part of the intermediate scattering function. These observations suggest that the NPLIN mechanism is not reliant on diffusion of solute, but rather on the reorganization of precritical amorphous clusters during the laser pulse, as in the TSN scenario.

An approach similar to DP has been proposed by Karpov and coworkers.[67–69] With appropriate parameters, it was shown that the decrease of the nucleation barrier for elongated metallic particles would be one or two orders of magnitude greater than with spherical dielectric particles, and this has a huge effect on the free energy profile predicted by CNT. Moreover, an estimate was made of the nucleation time (the rate of barrier crossing), and its effect on the required laser-pulse duration, which was assumed to be ~ 10 times as long to allow nucleation to occur. Additional effects considered in this work included plasmonic resonances driven by the laser, which could dominate over the static polarization; the greater stabilization of disk-like particles by CP light (similar to the OKE); and the possibility of melting of the metallic clusters.[68,69] Although such mechanisms would explain why realistic laser intensities have such a large effect on metastable solutions, there is no explanation for the origins of such metallic particles with high aspect ratios in the systems studied experimentally.

C. Nanoparticle heating

Theories of NPLIN based on the OKE and DP mechanisms are capable of explaining some of the experimental observations, but there are several significant and unresolved issues: (i) there is no adequate explanation for the threshold laser power; (ii) some systems do not exhibit NPLIN; (iii) filtration suppresses NPLIN to varying degrees; (iv) ultrafast pulses (~ 1 ps) do not effect NPLIN, despite higher peak electric fields; and (v) both the OKE and DP models predict a tiny reduction in the free-energy barrier to nucleation, at least at the electric field strengths employed in experiments. Many of these issues can be skirted, but only by introducing conditions that have little or no justification, such as enhanced polarizabilities due to structured clustering, or clusters with metallic properties. Worse than this, some of the experimental observations have been called into question. For example, needles of urea show no alignment with LP light, as first reported;[25] and polarization switching has been difficult to reproduce, being a much weaker effect than at first thought.[57]

With a view to resolving the issue of mechanism, Knott *et al.* found that NPLIN of carbon dioxide (CO_2) gas was possible.[46] In this system, the nucleated phase is a gas and hence $\epsilon_p < \epsilon_s$, which immediately rules out the DP mechanism. Experiments on shaking aqueous solutions supersaturated with respect to both glycine and argon suggested that the nucleation of gas bubbles facilitates nucleation of solids.

Ward *et al.* conducted a detailed study of NPLIN of aqueous sucrose solutions supersaturated with CO_2.[70] Curiously, the number of bubbles nucleated was found to increase quadratically with increasing laser intensity (above a threshold) rather than linearly as was found for NPLIN of solids. Both filtered and unfiltered samples were tested, and filtering reduced the lability by an order of magnitude. The threshold laser power (~ 4.7 MW cm^{-2}) remained constant for all samples, filtered or unfiltered, and was remarkably close to the values (~ 6 MW cm^{-2}) observed for NPLIN of the halides (see Section II C). The experiments showed that the number of bubbles nucleated increased approximately linearly with the sucrose concentration. Taken together with the results of filtration, this was a strong indication that the sucrose was introducing an impurity solid that activated NPLIN. Experiments employing rigorous measures to filter solutions and clean the glassware supported this indication. In a separate study, Navid *et al.* measured the nucleation induction times for both filtered and unfiltered samples of aqueous glycine solutions. They concluded that NPLIN was dependent on impurity particles.[29]

The NPLIN results for CO_2 were explained by a mechanism whereby a solid impurity nanoparticle is heated to a high temperature by the laser pulse, causing formation of a vapor cavity.[70] The vapor–solution interface acts as a seed for growth of a bubble by the influx of dissolved CO_2. It was suggested that formation of a vapor cavity may be also responsible for nucleation of solid crystals in NPLIN. Solute near a vapor-liquid interface may be less well solvated, and hence more likely to cluster and cause nucleation. Possible scenarios are illustrated schematically in Fig. 5.

The behavior of impurities in the solution raises the possibility of several different nucleation mechanisms, particularly if the impurities are highly absorbing, as this provides a means of energy transfer to the solution. The laser wavelengths, intensities, pulse durations, and total energies used in NPLIN experiments are more than sufficient to provide a significant perturbation to the solution structure. The effects of absorbent particles in pure liquids are interesting enough, let alone in solutions. For example, 100-nm carbon ink particles in water excited by 1064 nm laser pulses may be heated to temperatures of 2200 K, causing rapid heating of the surrounding water and bubble formation.[72,73] The subsequent pressurization of the surrounding liquid changes its refractive index, causing a transient optical grating which can be detected by light scattering. Crucially, the formation of bubbles around different particles occurs coherently, and more rapidly than would be expected by random nucleation. The explanation for this is that the water is beyond the spinodal temperature (~ 580 K) at which the liquid becomes absolutely unstable, and the vapor appears by spinodal decomposition at all of the particle-water interfaces simultaneously.

Plasmonic resonances in gold nanoparticle catalysts

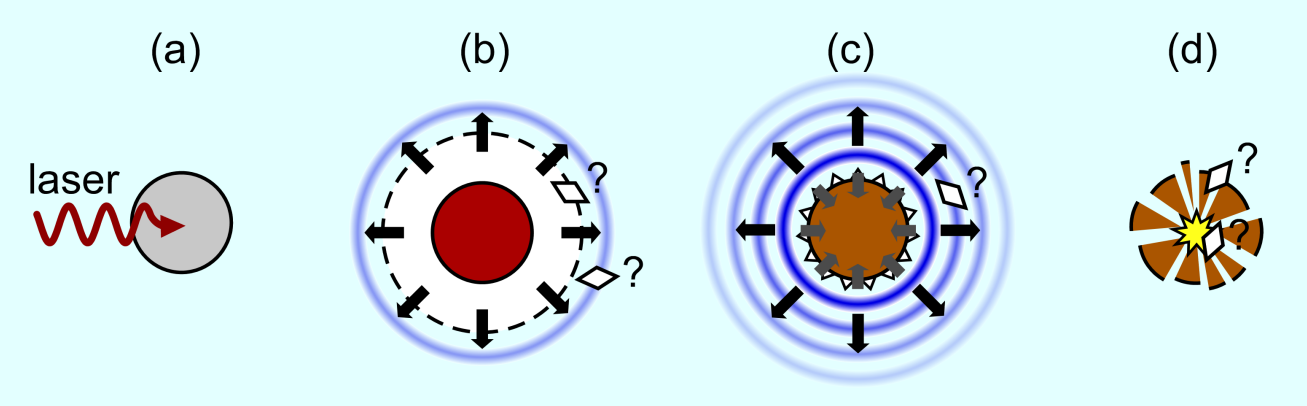

FIG. 5. Schematic diagrams illustrating possible scenarios for NPLIN of solids due to a particle-heating mechanism. The scenarios depicted here are not intended to represent an exhaustive list of options. (a) A nanoparticle absorbs energy from the laser pulse. (b) Rapid heating of the particle causes formation of an expanding vapor cavity, where it is possible nucleation occurs at the new interface; or in a region of increased concentration beyond the new interface, as suggested in MD simulations.[71] (c) Collapse of the vapor cavity causes outgoing pressure waves, where local increase in S causes nucleation. (d) Violent collapse of the vapor cavity results in destruction of the nanoparticle, possibly resulting in formation of a plasma, or inducing nucleation at fresh solid–liquid interfaces.

have been observed to cause local heating of water and bubble formation.[74–80] The structural evolution of the surfaces of gold nanoparticles and the immediate surrounding water following pulsed-laser excitation have been determined using X-ray scattering, and modeled using heat-transfer equations.[76] It has been shown that the nanoparticles may be heated to temperatures ~ 1000 K, and the local water temperature can increase by several hundreds of kelvin, causing bubble formation. Spinodal decomposition of water near gold nanodots has been confirmed directly by the observation of critical opalescence.[77] Bubble nucleation also has a feedback effect on the temperature of the nanoparticle. The growing vapor layer thermally insulates the nanoparticle from the surrounding liquid, meaning that the rate of heat dissipation decreases. This leads to a jump in the nanoparticle temperature.[79] Hydrodynamic models have been used to determine the ranges of nanoparticle size and laser intensity in which bubbles are formed and the nanoparticle melts.[81,82] Details of bubble dynamics on the picosecond-to-nanosecond timescale have been explored using pump-probe spectroscopy[80] and hydrodynamic modeling.[83]

Atomistic simulations of nanoparticle heating have been carried out. Sasikumar and Keblinksi carried out MD simulations of a heated solid nanoparticle in a Lennard-Jones liquid, and showed that bubble formation occurs when the surface of the nanoparticle is at around 90% of the critical temperature, i.e., beyond the spinodal temperature for this model.[84] Chen *et al.* explored the effects of model water potentials on simulations of a suspended gold nanoparticle,[85] and identified that the wettability of the particle surface, which is strongly affected by the choice of model, was a key factor in determining the heat transfer to the solution.[85]

To explore a particle-heating mechanism for NPLIN, the effect of a heated 2-nm nanoparticle on the structure of a supersaturated aqueous sodium chloride solution has been studied using atomistic MD simulations.[71] The nanoparticle was heated to a few thousand kelvin over ~ 10 ps. As well as the system expanding at constant pressure, the local salt *molality* was strongly depleted within 1.5–2.5 nm from the particle surface over 2–3 ns, and the ions became *more* clustered beyond that zone. Desolvation and clustering of ions could enhance the probability of nucleation. The threshold laser intensity might be dictated by the heating required to change the solution structure sufficiently.

Why not just do an MD simulation of NPLIN? The problems are twofold. Firstly, nucleation is a rare and stochastic event, whether induced by a laser pulse or not, and the challenges and specialized techniques for atomistic simulations are well documented.[86,87] Secondly, if the interaction between the laser and the solution is due to polarization rather than absorption, then a fully *ab-initio* MD technique would be required to accommodate the timescales of the laser (period ~ 1 fs), diffusion, pulse duration (~ 1 ns), and nucleation. This is a tall order, and to-date, simulations of NPLIN have been limited to simple models and an assumed *effect* of the laser light on the system, e.g., the OKE.[61]

Experimental estimates of the number of particles dispersed in supersaturated solutions lie in the range 10^6–10^8 cm^{-3}.[88] It is not clear whether these particles are mesoscale solute clusters, solid impurities, or a mixture of the two.[89] Results suggest that larger particles are more effective at causing NPLIN. The number of crystals (or bubbles) nucleated by a single laser pulse is typically in the range 1–100 cm^{-3}, meaning that the proportion of particles responsible for NPLIN is extremely low. It should come as no surprise, therefore, that even very pure reagents (< 10 ppm impurities) may result in multiple NPLIN events.

If solid impurities are responsible for NPLIN, the obvious question arises – what are these particles? Ward *et al.* filtered large volumes of nearly saturated aqueous ammonium chloride solution through 0.2 μm-pore membranes. The filter residue was digested by acid and analyzed using inductively coupled-plasma optical-emission

spectroscopy (ICP-OES) and mass spectrometry (ICP-MS).[42] The results indicated iron and phosphate as major components. Dynamic light-scattering measurements showed that the impurity particles were sub-micron in scale. Filtering of supersaturated solutions reduced the NPLIN lability; but by intentionally doping solutions with iron-oxide nanoparticles, this reduction could be reversed. It was also shown that long exposures (> 30 minutes, 10 Hz) to laser pulses at maximum power reduced NPLIN lability, presumably due to the destruction of particles.

As things stand, the evidence points to an NPLIN mechanism that depends upon trace impurity nanoparticles, rather than being an intrinsic effect of the electric field acting directly on solute clusters. What are the origins of the impurity particles in NPLIN-active systems? Sources might include the reactants during production of a compound, or particles accrued during processing, e.g., iron-oxide particles from stirring or grinding in contact with steel components. Other sources may be contaminants in the solvent or on the surfaces of the containers used. Being clean is easier said than done.

A nanoparticle-heating mechanism can explain several features of the NPLIN experiments that have otherwise evaded explanation. The essential features are summarized here, and the reader is directed elsewhere for details:[42,70] (i) the threshold laser power is observed because a threshold temperature is required to produce a vapor cavity; (ii) the wide ranges of impurity composition and concentration can explain the variability of NPLIN, and the differences in results between different studies; (iii) ageing effects may be explained by time-dependent aggregation of impurity nanoparticles; (iv) filtration suppresses NPLIN to varying degrees because impurities are removed; (v) heating depends on the total energy per pulse, which is higher for nanosecond than femtosecond laser pulses; (vi) thermodynamic estimates of the heating are commensurate with the rapid formation of micron-sized vapor cavities; and (vii) polarization switching may be explained by polarization-dependent optical absorption of the impurity nanoparticles.

IV. SHOCKWAVES AND CAVITY FORMATION

That mechanical shock can induce crystallization is widely known.[6] Corner a friendly chemist, and she or he will tell you that to grow large single crystals you should avoid disturbing your solution, and that scratching a glass vessel with a spatula can encourage nucleation. Ask them what is the reason, and you will receive a less-assured response. Perhaps pressure waves cause localized increases in supersaturation, which result in nucleation. Or maybe the cause is related to the formation of vapor bubbles by cavitation. Ultrasound is another method for inducing nucleation, known as sonocrystallization. It is known that, at appropriate frequencies and powers, ultrasound induces cavitation in liquids.[9] But, just as for nucleation by mechanical shock, the detailed mechanism for producing solid nuclei by sonocrystallization is uncertain.

Soare *et al.* and Jacob et al. studied crystal nucleation by laser-induced cavitation using focused laser pulses.[11,54] Compton and co-workers have studied nucleation by laser-induced pressure waves.[90,91] Laser pulses were focused onto a metal boat floating on the surface of a solution. Crystals were observed sedimenting down from the bottom of the boat, even though the light had not passed through the solution. The peak-power densities of pulses used (1.9 TW cm^{-2}) were several orders of magnitude higher than those employed in NPLIN studies. In the experiments on NPLIN of KCl in agarose gel, Duffus *et al.* noted that crystals were only formed where the light passed through the gel, and there was no evidence for transmission of pressure waves outside of the irradiated area.[40] Kacker *et al.* used a transducer to detect pressure waves produced during NPLIN of KCl at laser powers and conditions similar to those used in earlier work.[47,92] The laser was directed (unfocussed) onto a black mask on the outside of the glass vial. They concluded that the resulting shock waves transmitted into the solution were not responsible for NPLIN.

In order to compare NPLIN with sonocrystallization and mechanical shock, Liu *et al.* conducted a study on nucleation of supersaturated aqueous glycine.[57] They found that as S was increased from 1.4 to 1.7, the total fraction of samples nucleated increased linearly for NPLIN, but was relatively flat for the other two methods. The fraction of γ-glycine nucleated showed a sigmoidal dependence on S, tending to unity at high S. The similarity between the results for the different methods suggested cavitation as a common mechanism. The transition to γ-glycine at high S was sharper for NPLIN, which was attributed to cavitation events with higher energies, resulting in higher localized supersaturation, which favours γ-glycine.[59]

V. LOOKING FORWARD

Details of the mechanism for NPLIN are still being unraveled. Why is this the case? For one thing, the structures of concentrated solutions remains a hot topic for debate. Does a population of non-crystalline clusters exist in every solution? What are their sizes, structures, and dynamics? The measurement of subnanometer length-scale processes, occurring on subnanosecond timescales, and among a sea of species that look similar, is challenging to put it mildly. That NPLIN is dependent on rare events involving low-concentration impurities should not come as a surprise, and homogeneous nucleation no doubt happens less often than is assumed.

The dependence of NPLIN on impurity nanoparticles opens several avenues for the further study and control of nucleation. Apart from NPLIN, studies of laser heating of particles have focused heavily on gold nanoparticles, due to their metallic character, and strong plasmon resonances in the visible to near-infrared spectrum. Laser heating of other nanoparticles, such as iron oxides, should be studied in more detail to explore absorption and heat-transfer characteristics. It may be possible to tailor nanoparticles to promote nucleation in sys-

tems that do not exhibit NPLIN, or to direct nucleation of desired polymorphs. This underlines an exciting and promising future for the field, e.g., generating novel morphologies such as nanocrystals, or producing crystals of materials that are much needed but difficult to obtain, such as proteins for structural analysis by X-ray or neutron diffraction.

At present, it would be fair to say that the evidence for the polarization switching effect is still patchy. More experiments are required to nail this down, with improved statistics and better control experiments. Of particular interest is how bias in the nucleation of polymorphs can be effected. For example, in the aqueous glycine system, it is not at all clear why nucleation of α-glycine is favored at low S, and γ-glycine at high S.

If the rapid heating of impurity nanoparticles causes NPLIN of solids, is the formation of a vapor–liquid interface necessary, or is it due to the resulting pressure waves, or something else? The recent MD simulations show tantalizing evidence for solute clustering in the proximal region of solution just outside a rarified cavity.[71] In the coming years, NPLIN promises to yield a rich seam of novel and interesting chemical physics that can be mined by a dual approach combining experiment and simulation. And in doing so, we hope that many new aspects of nucleation in general may be discovered.

ACKNOWLEDGMENTS

The authors acknowledge support from the Engineering and Physical Sciences Research Council EPSRC through funding for some of the work described in this Perspective (EP/G067546/1, EP/I033459/1 and EP/L022397/1). PJC acknowledges support from the Ministry of Education and Science of the Russian Federation (Agreement no. 02.A03.21.0006, Project no. 3.1438.2017/4.6). We are grateful to our colleagues, collaborators, reviewers, and editors for their encouragement and suggestions over the years.

[1] J. W. Mullin, *Crystallization* (Butter-Heinemann, Oxford, 2001).
[2] I. V. Markov, *Crystal growth for beginners: fundamentals of nucleation, crystal growth, and epitaxy*, 2nd ed. (World Scientific, Singapore, 2003).
[3] D. Erdemir, A. Y. Lee, and A. S. Myerson, Acc. Chem. Res. **42**, 621 (2009).
[4] P. G. Vekilov, Cryst. Growth Des. **10**, 5007 (2010).
[5] D. Gebauer, A. Völkel, and H. Cölfen, Science **322**, 1819 (2008).
[6] S. W. Young, J. Am. Chem. Soc. **33**, 148 (1911).
[7] Z. Hammadi and S. Veesler, Progress in Biophysics and Molecular Biology **101**, 38 (2009).
[8] A. E. Dubinov, J. P. Kozhayeva, I. L. L'vov, S. A. Sadovoy, V. D. Selemir, and D. V. Vyalykh, Crystal Growth & Design **15**, 4975 (2015).
[9] M. L. de Castro and F. Priego-Capote, Ultrasonics Sonochemistry **14**, 717 (2007).
[10] B. A. Garetz, J. E. Aber, N. L. Goddard, R. G. Young, and A. S. Myerson, Phys. Rev. Lett. **77**, 3475 (1996).
[11] A. Soare, R. Dijkink, M. R. Pascual, C. Sun, P. W. Cains, D. Lohse, A. I. Stankiewicz, and H. J. M. Kramer, Crystal Growth & Design **11**, 2311 (2011).
[12] T. Sugiyama, K.-i. Yuyama, and H. Masuhara, Accounts of Chemical Research **45**, 1946 (2012).
[13] T. Sugiyama, T. Adachi, and H. Masuhara, Chemistry Letters **36**, 1480 (2007).
[14] R. G. Young, *Laser Interactions with Supersaturated Urea Solutions*, B.S. thesis, Polytechnic University (1994).
[15] L. Kou, D. Labrie, and P. Chylek, Appl. Opt. **32**, 3531 (1993).
[16] A. Tam, G. Moe, and W. Happer, Phys. Rev. Lett. **35**, 1630 (1975).
[17] N. Nakashima, H. Inoue, M. Sumitani, and K. Yoshihara, The Journal of Chemical Physics **73**, 4693 (1980).
[18] J. Matic, X. Sun, B. A. Garetz, and A. S. Myerson, Cryst. Growth Des. **5**, 1565 (2005).
[19] J. Matic, X. Sun, B. A. Garetz, and A. S. Myerson, Crystal Growth & Design **5**, 1565 (2005).
[20] A. D. Buckingham, Proc. Phys. Soc. B **69**, 344 (1956).
[21] P. D. Maker, R. W. Terhune, and C. M. Savage, Phys. Rev. Lett. **12**, 507 (1964).
[22] G. Mayer and F. Gires, C. R. Hebd. Séances Acad. Sci. **258**, 2039 (1964).
[23] M. A. Duguay and J. W. Hansen, Appl. Phys. Lett. **15**, 192 (1969).
[24] P. P. Ho and R. R. Alfano, Phys. Rev. A **20**, 2170 (1979).
[25] Y. Liu, M. R. Ward, and A. J. Alexander, Phys. Chem. Chem. Phys. **19**, 3464 (2017).
[26] J. Zaccaro, J. Matic, A. S. Myerson, and B. A. Garetz, Cryst. Growth Des. **1**, 5 (2001).
[27] J. Matić, *Non-photochemical light-induced nucleation and control of polymorphism through polarization-switching*, Ph.D. thesis, Polytechnic University (2005).
[28] A. J. Alexander and P. J. Camp, Cryst. Growth Des. , 958 (2009).
[29] N. Javid, T. Kendall, I. S. Burns, and J. Sefcik, Crystal Growth & Design **16**, 4196 (2016).
[30] B. A. Garetz, J. Matic, and A. S. Myerson, Phys. Rev. Lett. **89**, 175501 (2002).
[31] D. W. Oxtoby, Nature **420**, 277 (2002).
[32] L. F. Power, K. E. Turner, and F. H. Moore, Acta Cryst. **B32**, 11 (1976).
[33] Å. Kvick, W. M. Canning, T. F. Koetzle, and G. J. B. Williams, Acta Cryst. **B36**, 115 (1980).
[34] "Avogadro: an open-source molecular builder and visualization tool. Version 1.2.0," `http://avogadro.cc/` (2018).
[35] M. D. Hanwell, D. E. Curtis, D. C. Lonie, T. Vandermeersch, E. Zurek, and G. R. Hutchison, J. Cheminformatics **4**, 17 (2012).
[36] B. D. Bean, personal communication.
[37] K. Fang, S. Arnold, and B. A. Garetz, Cryst. Growth Des. **14**, 2685 (2014).
[38] M. R. Ward and A. J. Alexander, Cryst. Growth Des. **12**, 4554 (2012).
[39] M. R. Ward, I. Ballingall, M. L. Costen, K. G. McKendrick, and A. J. Alexander, Chem. Phys. Lett. **481**, 25 (2009).
[40] C. Duffus, P. J. Camp, and A. J. Alexander, Journal of the American Chemical Society **131**, 11676 (2009).
[41] M. R. Ward, A. Rae, and A. J. Alexander, Cryst. Growth Des. **15**, 4600 (2015).
[42] M. R. Ward, A. M. Mackenzie, and A. J. Alexander, Cryst. Growth Des. **16**, 6790 (2016).
[43] B. Clair, A. Ikni, W. Li, P. Scouflaire, V. Quemener, and A. Spasojević-de Biré, Journal of Applied Crystallography **47**, 1252 (2014).
[44] A. Ikni, B. Clair, P. Scouflaire, S. Veesler, J.-M. Gillet, N. El Hassan, F. Dumas, and A. Spasojević-de Biré, Crystal Growth & Design **14**, 3286 (2014).
[45] X. Sun, B. A. Garetz, M. F. Moreira, and P. Palffy-Muhoray, Phys. Rev. E **79**, 021701 (2009).
[46] B. C. Knott, J. L. LaRue, A. M. Wodtke, M. F. Doherty, and B. Peters, J. Chem. Phys. **134**, 171102 (2011).
[47] M. R. Ward, S. McHugh, and A. J. Alexander, Phys. Chem. Chem. Phys. **14**, 90 (2012).
[48] M. R. Ward, G. W. Copeland, and A. J. Alexander, J. Chem. Phys. **135**, 114508 (2011).
[49] I. S. Lee, J. M. B. Evans, D. Erdemir, A. Y. Lee, B. A. Garetz, and A. S. Myerson, Crystal Growth & Design **8**, 4255 (2008).
[50] N. Yennawar, S. Denev, V. Gopalan, and H. Yennawar, Acta Crystallographica Section F **66**, 969 (2010).
[51] M. P. Arciniegas, A. Castelli, S. Piazza, S. Dogan, L. Ceseracciu, R. Krahne, M. Duocastella, and L. Manna, Advanced Functional Materials **27**, 1701613 (2017).

[52]Z. Liu and C. R. Liu, Nanoscale **10**, 14400 (2018).
[53]H. Adachi, K. Takano, Y. Hosokawa, T. Inoue, Y. Mori, H. Matsumura, M. Yoshimura, Y. Tsunaka, M. Morikawa, S. Kanaya, H. Masuhara, Y. Kai, and T. Sasaki, Japanese Journal of Applied Physics **42**, L798 (2003).
[54]J. A. Jacob, S. Sorgues, A. Dazzi, M. Mostafavi, and J. Belloni, Crystal Growth & Design **12**, 5980 (2012).
[55]X. Sun, B. A. Garetz, and A. S. Myerson, Crystal Growth & Design **8**, 1720 (2008).
[56]W. Li, A. Ikni, P. Scouflaire, X. Shi, N. El Hassan, P. Gémeiner, J.-M. Gillet, and A. Spasojević-de Biré, Crystal Growth & Design **16**, 2514 (2016).
[57]Y. Liu, M. H. van den Berg, and A. J. Alexander, Phys. Chem. Chem. Phys. **19**, 19386 (2017).
[58]F. Walton and K. Wynne, Nature Chemistry **10**, 506 (2018).
[59]K.-i. Yuyama, T. Rungsimanon, T. Sugiyama, and H. Masuhara, Crystal Growth & Design **12**, 2427 (2012).
[60]X. Sun, B. A. Garetz, and A. S. Myerson, Cryst. Growth Des. **6**, 684 (2006).
[61]B. C. Knott, M. F. Doherty, and B. Peters, J. Chem. Phys. **134**, 154501 (2011).
[62]J. O. Isard, Philos. Mag. **35**, 817 (1977).
[63]V. B. Warshavsky and A. K. Shchekin, Colloids Surf. A **148**, 283 (1999).
[64]M. D. Cohen, R. C. Flagan, and J. H. Seinfeld, J. Phys. Chem. **91**, 4583 (1987).
[65]B. C. Knott, N. Duff, M. F. Doherty, and B. Peters, J. Chem. Phys. **131**, 224112 (2009).
[66]J. O. Sindt, A. J. Alexander, and P. J. Camp, J. Phys. Chem. B **118**, 9404 (2014).
[67]V. G. Karpov, M. Nardone, and N. I. Grigorchuk, Phys. Rev. B **86**, 075463 (2012).
[68]M. Nardone and V. G. Karpov, Phys. Chem. Chem. Phys. **14**, 13601 (2012).
[69]N. I. Grigorchuk and V. G. Karpov, Appl. Phys. Lett. **105**, 223103 (2014).
[70]M. R. Ward, W. J. Jamieson, C. A. Leckey, and A. J. Alexander, J. Chem. Phys. **142**, 144501 (2015).
[71]J. O. Sindt, A. J. Alexander, and P. J. Camp, J. Chem. Phys. **147**, 214506 (2017).
[72]K. J. McEwan and P. A. Madden, J. Chem. Phys. **97**, 8748 (1992).
[73]H. Löwen and P. A. Madden, J. Chem. Phys. **97**, 8760 (1992).
[74]J. R. Adleman, D. A. Boyd, D. G. Goodwin, and D. Psaltis, Nano Lett. **9**, 4417 (2009).
[75]E. Lukianova-Hleb, Y. Hu, L. Latterini, L. Tarpani, S. Lee, R. A. Drezek, J. H. Hafner, and D. O. Lapotko, ACS Nano **4**, 2109 (2010).
[76]A. Siems, S. A. L. Weber, J. Boneberg, and A. Plech, New J. Phys. **13**, 043018 (2011).
[77]M. T. Carlson, A. J. Green, and H. H. Richardson, Nano Lett. **12**, 1534 (2012).
[78]Z. Qin and J. C. Bischof, Chem. Soc. Rev. **41**, 1191 (2012).
[79]Z. Fang, Y.-R. Zhen, O. Neumann, A. Polman, F. J. G. de Abajo, P. Nordlander, and N. J. Halas, Nano Lett. **13**, 1736 (2013).
[80]T. Katayama, K. Setoura, D. Werner, H. Miyasaka, and S. Hashimoto, Langmuir **30**, 95049513 (2014).
[81]J. Lombard, T. Biben, and S. Merabia, Phys. Rev. Lett. **112**, 105701 (2014).
[82]J. Lombard, T. Biben, and S. Merabia, Phys. Rev. E **91**, 043007 (2015).
[83]J. Lombard, T. Biben, and S. Merabia, J. Phys. Chem. C **121**, 15402 (2017).
[84]K. Sasikumar and P. Keblinski, J. Chem. Phys. **141**, 234508 (2014).
[85]X. Chen, A. Munjiza, K. Zhang, and D. Wen, J. Phys. Chem. C **118**, 1285 (2014).
[86]V. Agarwal and B. Peters, Adv. Chem. Phys. **155**, 97 (2014).
[87]G. C. Sosso, J. Chen, S. J. Cox, M. Fitzner, P. Pedevilla, A. Zen, and A. Michaelides, Chem. Rev. **116**, 70787116 (2016).
[88]M. R. Ward, S. W. Botchway, A. D. Ward, and A. J. Alexander, Faraday Discuss. **167**, 441 (2013).
[89]A. Jawor-Baczynska, J. Sefcik, and B. D. Moore, Cryst. Growth Des. **13**, 470 (2013).
[90]A. Fischer, R. M. Pagni, R. N. Compton, and D. Kondepudi, in *Nanoclusters*, edited by P. Jena and A. Castleman, Jr. (Elsevier, Amsterdam, 2010) Chap. 8, pp. 343–364.
[91]N. Mirsaleh-Kohan, A. Fischer, B. Graves, M. Bolorizadeh, D. Kondepudi, and R. N. Compton, Cryst. Growth Des. **17**, 576 (2017).
[92]R. Kacker, S. Dhingra, D. Irimia, M. K. Ghatkesar, A. Stankiewicz, H. J. M. Kramer, and H. B. Eral, Cryst. Growth Des. **18**, 312 (2018).